Auger Electron Emission from Clean and Carbon-Contaminated Mo†

DENNIS W. VANCE
Xerox Research Laboratories, Rochester, New York
(Received 26 June 1967)

Measurements have been made of the Auger electron yield from polycrystalline Mo targets bombarded by mass-selected beams of Ar^+ and He^+ ions at normal incidence. The yields were measured for incident-ion kinetic energies of 50–400 eV. The experiments were conducted in ultrahigh vacuum to insure well-defined surface conditions. It was found that atomically clean Mo surfaces could not be produced by heating the targets to 2300°K, but that carbon impurities diffusing from the bulk of the sample accumulated at the surface and were not removed by heating. The carbon-contaminated surfaces gave reduced electron yields for both ions. This effect is thought to explain discrepancies among experimental results previously reported in the literature. The carbon contamination was removed by heating the target in O_2, and it is argued that the resulting surface is atomically clean. The measured thermionic work function of the carbon-covered surface was 0.4 eV greater than the clean-surface value.

INTRODUCTION

THE study of electron emission due to rare-gas ion bombardment of refractory metals has received a great deal of attention in the literature.[1–3] Unfortunately, a large portion of the work prior to about 1950 was done with poorly controlled surface conditions and hence cannot be clearly interpreted. Recently, experimental techniques have progressed to the point where surfaces can be prepared and maintained in a known state of cleanliness.

Electron emission produced by ion bombardment of clean metal surfaces proceeds by two distinguishable mechanisms. For ion kinetic energies below about 500 eV, ejection of electrons occurs primarily by the potential or Auger mechanism. This process can be regarded as an electronic state transition of the system metal plus ion resulting in a neutral atom and the removal of two electrons from the metal. Higher-energy ions eject electrons by the so-called "kinetic" mechanism, in which bound electrons in the metal are accelerated in collisions between incident ions and lattice atoms where appreciable momentum is transferred. Kinetic ejection from clean metal surfaces is negligible for ion energies below a threshold energy, usually of the order of several hundred volts. Most of the experimental results reported in the literature deal with ion energies in the kinetic ejection region. A notable exception is the very extensive research program conducted by Hagstrum and co-workers over the past 15 years,[4–7] in which they have examined the interaction of rare-gas ions with a variety of metal and semiconductor surfaces. The only results which can be considered comparable to Hagstrum's are the investigations of Mahadevan *et al*[8] (He^+, Ar^+, on Mo) and of Propst and Luscher[9] (He^+ on W). Despite the similar procedures used by all of these investigators, large discrepancies exist in the results, particularly in the case of Ar^+ on Mo.

We have made measurements of the yield γ_i of secondary electrons ejected from polycrystalline Mo targets bombarded by Ar^+ and He^+ in the energy range 50–400eV. Results of previous investigators have been reproduced and the discrepancies are shown to be a result of the failure of target heating alone to remove carbon from the surface of the target. Heating in O_2 produces a surface which gives Hagstrum's yield values, presumably referring to an atomically clean surface. The crystallinity and degree of orientation of the target are considered with the aid of x-ray analysis. A model of the carbon contaminated surface is presented which is consistent with the differences in electron yield measured for the clean and contaminated surfaces.

APPARATUS

The apparatus used in this work is new and has not been previously described. Basically, it consists of an ion source, a mass selector, and a target and collector system enclosed in an ultra high vacuum system. Differential pumping prevents ion source gas from contaminating the target surface. The apparatus is shown schematically in Fig. 1. The various sections will be described separately below.

Ion Source

The ion source is of the electron-bombardment type.[10] The gas to be ionized is introduced in the form of a

† This material presented, in part, at the XXVII Annual Conference on Physical Electronics, Cambridge, Massachusetts, March, 1967.

[1] The work prior to about 1950 is reviewed in H. S. W. Massey and E. H. S. Burhop, *Electronic and Ionic Impact Phenomena* (Oxford University Press, London, 1956), Chap. 9.

[2] A more recent survey is that of M. Kaminsky, *Atomic and Ionic Impact Phenomena on Metal Surfaces* (Academic Press Inc., New York, 1965).

[3] Kinetic ejection is reviewed by B. Medved and Y. E. Strausser, in *Advances in Electronics and Electron Physics*, edited by L. Marton (Academic Press Inc., New York, 1965), Vol. 21, p. 101.

[4] H. D. Hagstrum, Phys. Rev. **104**, 672 (1956).

[5] H. D. Hagstrum, Phys. Rev. **89**, 244 (1953).

[6] H D. Hagstrum, Phys. Rev. **104**, 1516 (1956).

[7] H. D. Hagstrum, Phys. Rev. **150**, 495 (1966).

[8] P. Mahadevan, J. K. Layton, and D. B. Medved, Phys. Rev. **129**, 79 (1963).

[9] F. M. Propst and E. Luscher, Phys. Rev. **132**, 1037 (1963).

[10] D. W. Vance and T. L. Bailey, Rev. Sci. Instr. **34**, 925 (1963).

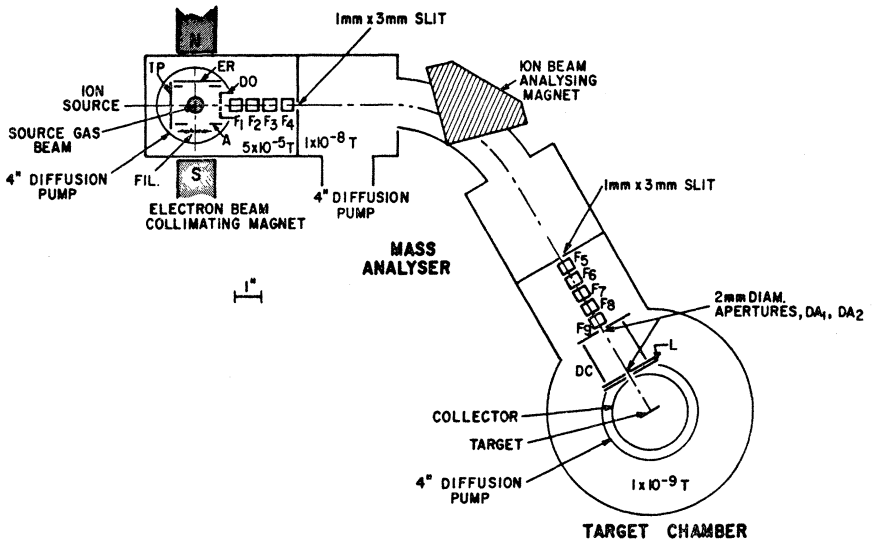

FIG. 1. Schematic diagram of apparatus. The source gas beam is directed into the plane of the figure.

dense molecular beam at right angles to the plane of a ribbon-shaped electron beam and the axis of the ion focusing system. The molecular beam is formed by introducing the gas through an array of parallel channels,[11] and is directed into the throat of a 4-in. liquid-nitrogen trapped oil diffusion pump. This arrangement allows the attainment of relatively high pressures ($\sim 10^{-3}$ Torr) in the region of intersection of the gas and electron beams while reducing gas flow into the ion focusing system and subsequent vacuum chambers. Electrons are emitted by the directly heated filament, Fil, and are accelerated by the anode A. The operation of the elements IP (ion pusher) and ER (electron reflector) are described in detail in Ref. 10. In order to avoid complications due to metastable ions, electron energies less than 30 eV are used to produce Ar^+ ions. He^+ ions are produced with 100 eV electrons. It has been established that few He^+ metastables are produced under these conditions.[4] The ions formed are extracted by a small electric field established between the elements, DO and IP, and are focused and accelerated by a series of four coaxial bipotential cylinder lenses, F_1 through F_4.

Mass Selector

The mass selector is a 60° magnetic deflection device employing the inflection-focusing principle.[12] This reduces the drift-tube lengths and provides second-order direction focusing of the ions, thus increasing the transmission of the instrument. The deflecting magnetic field is produced by an external electromagnet. The shape of the pole face of the magnet producing the inflection field is shown by the shaded area in the figure. The entrance and exit apertures of the instrument are slits, 1×3 mm and the mean radius of curvature of the ion path is 10 cm. The instrument is capable of fully separating adjacent masses up to about mass 30.

The ions pass through the mass analyzer at a fixed energy of about 200 eV. The second series of cylinder lenses, F_5 through F_9 are used to accelerate or decelerate the mass-analyzed beam to the desired interaction energy while focusing the beam onto the target.

Target and Collector System

The target and collector system are shown in detail in Fig. 2.

The target-collector geometry is similar to that commonly employed in experiments of this type, the midpoint of the ribbon-shaped target lying at the center of a spherical collector. The ion beam is collimated by the 2-mm-diam apertures DA_1 and DA_2 and the intervening space is shielded from stray electric fields by the cylinder DC. The elements DA_1, DA_2, and DC are all maintained at target potential. The half-angle of divergence of the beam is geometrically restricted to less than 2°. This prevents the beam from striking the element L of the exterior of the collector sphere C. Neglecting the small focusing effect of L, the cross-sectional diameter of the beam in the target plane is restricted to less than 4 mm. An elaborate alignment procedure insures that the mass-spectrometer slits, ion lenses, and collimating apertures are coaxial. All electrode surfaces exposed to the ion beam are sandblasted and gold plated to reduce beam instability due to surface charging. Typical currents to the target are $\sim 10^{-9}$ A. The total energy spread in the beam is of the order of 1 eV. The element L, an aperture lens, is held a few volts negative with respect to DA_2, thereby preventing electrons produced by ions striking DA_2 from reaching the collector, and also preventing electrons from the target from escap-

[11] J. A. Giordmaine and T. C. Wang, J. Appl. Phys. **31**, 463 (1960).
[12] H. Hintenberger, Rev. Sci. Instr. **20**, 855 (1949).

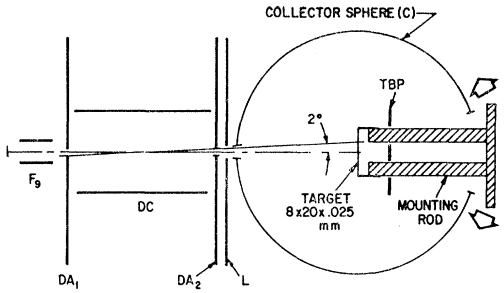

FIG. 2. Detailed schematic diagram of target and collector system.

ing through the beam entrance aperture in C. In practice, it was found that the potential of the L electrode had very little influence on the results except at the lowest energies where large positive potentials of L with respect to DA_2 would defocus the beam, causing it to strike the exterior of the collector. This insensitivity to L demonstrates that the collector current is negligibly affected by processes occurring outside the sphere entrance aperture. The target is in the form of a polycrystalline ribbon of dimensions indicated in Fig. 2. It is mounted on heavy copper rods in a holder which can be rotated by means of an externally controlled gearing system. The target normal may be rotated through angles from $-10°$ to $+60°$ with respect to the incident ion beam. All measurements to be reported in this paper are for normal incidence of the ion beam. The target may be directly heated for cleaning by an ac current of up to 60 A from a low-voltage transformer. The current to a small electrode behind the target (TBP in Fig. 2) is measured under various conditions to insure that all the ions entering the sphere strike the target. At all times, the current to this element is less than 10^{-14} A. The target ribbon may be viewed directly through a glass port on the target chamber. The temperature of the target is measured with an optical pyrometer and standard-emissivity and window-attenuation corrections are applied.[13]

Vacuum System

The entire apparatus is constructed of bakable materials. The vacuum envelope is type-304 stainless steel. Copper gasketed shear-type flanges are used throughout. Electrode parts are mounted on stainless rods using spacers of Pyrex and of sintered Alumina. The collector sphere is gold-plated copper.

The ion source, mass analyzer, and target are enclosed in separately pumped vacuum chambers interconnected only by the 1×3mm analyzer apertures. A 4-in. oil-diffusion pump is used on the ion-source chamber and 4-in. mercury-diffusion pumps are used on the analyzer and target chambers. Anticreep liquid-nitrogen traps are employed on all pumps. Fore vacuum is maintained by two zeolite trapped two-stage rotary mechanical pumps.

[13] *American Institute of Physics Handbook* (McGraw Hill Book Company, Inc., New York, 1963), 2nd ed., pp. 6–153.

EXPERIMENTAL PROCEDURES

Current Measurements

Secondary electrons, ions, and neutral particles resulting from the interaction of the ions with the target surface move radially outward toward the collector sphere. By applying a positive potential to the sphere, the flux of secondary electrons can be separated from the positive ions and neutral particles. Figure 3 shows a typical current-voltage characteristic obtained by varying the collector potential V_c and measuring the target and collector currents, I_t and I_c. The quantity $I=I_c/(I_c+I_t)$ is the normalized collector current, I_c+I_t being the total current entering the sphere. For positive values of V_c with respect to the target, I saturates at the negative value I^*. In this saturation region, the sphere current is composed of secondary electrons from the target as well as reflected ions with sufficient energy to surmount the potential barrier presented by the collector. As V_c is made negative, the secondary electrons are retarded and I saturates at the positive value R. The composition of this current is quite complex, since it may include reflected ions as well as tertiary electrons produced at the sphere surface which are collected on the target. The value of the secondary electron yield, γ_i will thus be given by I^* minus the ratio $R_i=I_i/(I_c+I_t)$, where I_i is the reflected ion current. R_i cannot be separated from the other components of R in this experiment, but clearly R_i cannot exceed R. Thus, the true value of γ_i will lie between I^* and I^*-R. In the present work, R is always less than 2% of I^* and has been neglected. Hagstrum has examined the component currents in R and has shown that about $\frac{1}{2}$ of the observed current is due to reflected ions,[14] the remainder being due to secondary

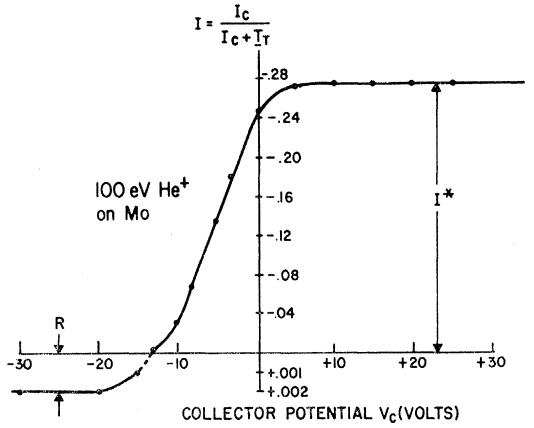

FIG. 3. Collector current-voltage characteristic obtained for 100 eV He^+ bombarding clean Mo. The quantities I^* and R are discussed in the text. Note the scale change for positive values of I.

[14] H. D. Hagstrum, Phys. Rev. **123**, 758 (1961).

electrons produced at the sphere. Hence, our neglect of R results in less than 1% error in γ_i.

Vacuum Procedures

The apparatus, exclusive of the pumps and traps, is baked at temperatures up to 500°K with a large oven. Baking is usually maintained for about 6 h with the traps cold and the target at ~1600°K. The oven is then turned off and the system is allowed to cool with the target hot. Finally, the target is turned off and the electrodes near the target are allowed to cool. This treatment lowers the pressure throughout the apparatus to $\sim 2\times 10^{-9}$ Torr as measured on ion gauges. The pressure decreases very slowly with time after bakeout. A mass-spectral analysis of the residual gases in the target chamber after baking indicated a large mercury peak, with smaller peaks at masses 18, 28, and 44. If a large portion of the residual gas is mercury, then the true total pressure must be of the order of 10^{-9} Torr or less.

Pressures in the various chambers under operating conditions with the source gas on and the ion beam striking the target are as indicated on Fig. 1. The partial pressure of source gas in the target chamber was always less than 10^{-9} Torr.

After the initial bakeout of the system, it was found that acceptable vacua could be obtained without an over-all bakeout of the apparatus by using the hot target as an internal heater. The system was pumped for about two days with the target at 1600°K. After allowing the system to cool, the pressure was 5×10^{-9} Torr and gradually decreased over a period of a few days. Results obtained after this treatment did not differ from those obtained after a full bakeout as described above.

Target Preparation and Cleaning

Targets were cut from 1-mil rolled molybdenum foil. The stated purity was 99.95%, but no detailed analysis of impurity content was available.[15] The targets were ultrasonically cleaned in successive baths of detergent, distilled water, and ethanol. X-ray analysis of the target material as installed in the apparatus, before heating, showed targets were preferentially oriented with the (100) face exposed.

The target surface was cleaned by rapid heating (flashing) to high temperatures (~2300°K). The flashing current was abruptly turned on, causing the target to heat to the maximum temperature in about 1 sec. The current was maintained for a short period and then switched off, allowing the target to cool in a few seconds. Under normal vacuum conditions, flashing the target in this manner resulted in a pressure pulse of the order of $\frac{1}{2}$-sec duration as measured on an ion gauge and oscilloscope. The pressure returned immediately to the base pressure after the pulse and remained

[15] Material supplied by A. D. Mackay Inc., New York.

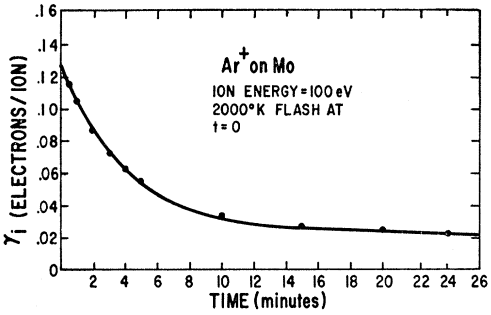

FIG. 4. Variation of γ_i with time after flash for 100-eV Ar^+ incident on clean Mo.

there. If the target was held at the flashing temperature for a long time, the pressure slowly rose, beginning several minutes after the initiation of the heating cycle, due to radiative heating and outgassing of the collector sphere. It was found that maintaining the flashing current for a period of 15 sec was sufficient to remove adsorbed gas without detectable readsorption upon cooling or appreciable background-pressure rise due to radiative heating.

It is well known that the process of Auger electron ejection is extremely sensitive to surface conditions. Hagstrum has studied the effect of adsorption of a monolayer of gas molecules on the secondary emission yield from clean tungsten surfaces.[6] He finds the monolayer adsorption of N_2, CO, or H_2 decreases γ_i for all rare-gas ions at all energies. The rate at which a clean metal surface will become contaminated by adsorption of molecules from the ambient atmosphere is determined by the pressure of the gas and the probability of sticking. Figure 4 shows the variation of γ_i with time after cleaning the target by flashing for 15 sec at 2000°K. The background pressure was about 4×10^{-9} Torr ion gauge pressure. The rapid initial decrease in γ_i followed by a transition to a much smaller rate of change in about 10 min reflects the effect of adsorption of gas on the target. A number of investigators, beginning with the work of Becker and Hartman,[16] have shown the adsorption of gas on a clean metal surface follows a curve which is the "reflection" of Fig. 4. That is, the adsorption rate begins at a high initial value and then decreases to a much lower value in a time which is identified with the time required to form a monolayer of gas on the surface.

If it is assumed that adsorption takes place on definite sites and that the sticking probability is α for an open site and zero for an occupied site, then the fractional number of occupied sites at any time t is given by

$$N(t)/N_0 = 1 - \exp(-\alpha I_0 t), \qquad (1)$$

where N_0 is the total number of adsorption sites and I_0 is the rate of incidence of adsorbable molecules. If

[16] J. A. Becker and C. D. Hartman, J. Phys. Chem. 57, 153 (1953).

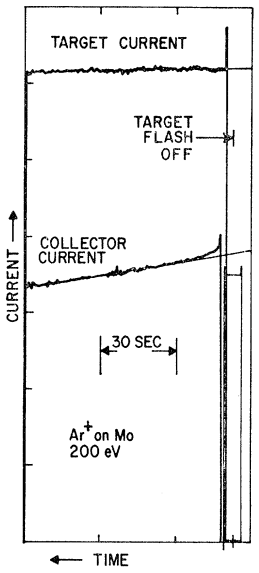

FIG. 5. Tracing of actual recorder output showing I_c and I_t as a function of time after flash.

it is further assumed[8] that the Auger electron emission yield from an occupied site is γ_1 and that from an unoccupied site is γ_2, this leads to

$$\gamma_i(t) = \gamma_1 + (\gamma_2 - \gamma_1) e^{-\beta t}, \quad (2)$$

where $\beta = \alpha I_0$. For small values of βt, i.e., values of t much less than the monolayer formation time, Eq. (2) becomes

$$\gamma_i(t) = \gamma_2 - (\gamma_2 - \gamma_1)\beta t, \quad (3)$$

a linear function of time with an intercept equal to the clean-surface value of γ_i. This provides a particularly simple means of obtaining $\gamma_2 = \gamma_i(0)$. By means of a system of relays, the collector and target currents can be displayed continuously on a chart recorder beginning about 3 sec after the flashing currrent is turned off. Figure 5 shows such a recorder trace. The initial linear portions of the curves can be extrapolated as indicated to yield the values of I_c and I_t at $t=0$. All of the values of γ_i reported in this paper were computed from currents obtained by this extrapolation technique.

The question remains: Is the surface produced by flashing the target to a given temperature atomically clean?

The most direct evidence bearing on this question is derived from the low-energy electron diffraction (LEED) work of Haas and Jackson[17] on the (110) face of molybdenum single crystals. They find that heating the crystal to 2000°K does not produce a clean Mo (110) pattern. They conclude by analogy with Stern's[18] similar results on W (110) that the fractional order beams observed are due to impurity carbon which diffuses to the surface from the bulk during heating and accumulates there. Stern used a mass spectrometer to show that the impurity was indeed carbon. Similar results have been obtained by Taylor[19] on W (111) and Estrup and Anderson[20] on W (100). In all cases, it was found that the carbon pattern could not be removed by heating even to temperatures near the melting point of the material. However, in all cases, it was found that heating the contaminated crystal in O_2 removed the carbon and produced the LEED pattern characteristic of the clean substrate. This observation is in accordance with the earlier work of Schlier[21] and of Becker *et al.*,[22] who investigated the production of CO during heating in O_2 of polycrystalline tungsten filaments containing carbon impurities. In the work of Haas and Jackson, "several" treatments of 10 min at 10^{-6} Torr of O_2 and 1200°K were found to be sufficient to remove the carbon. After carbon removal, the clean-surface pattern could always be produced from a surface covered with an adsorbed layer by heating the sample to 1900°K or less. These results refer to (110) Mo surfaces, whereas our "polycrystalline" target was found to be composed of oriented crystallites

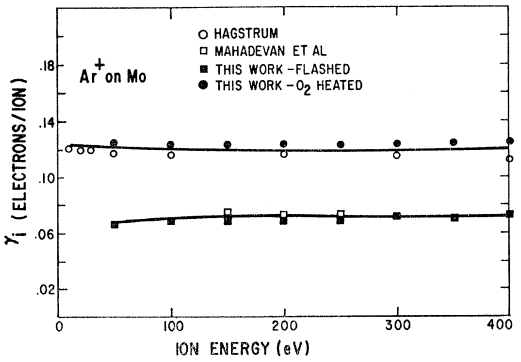

FIG. 6. Variation of γ_i with ion energy for Ar^+. Target treatments denoted "flashed" and "O_2-heated" are described in the text. The results of Hagstrum and Mahadevan are obtained from Refs. 4 and 8, respectively. The points due to Mahadevan coincide with the present measurements above 300 eV.

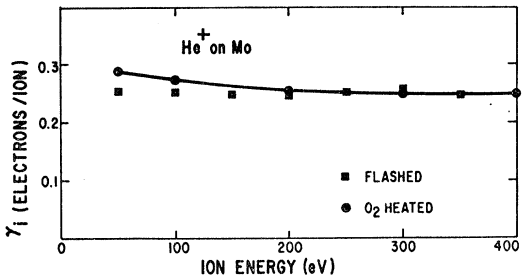

FIG. 7. Variation of γ_i with ion energy for He^+. The target treatments denoted "flashed" and "O_2-heated" are discussed in the text. The points due to Hagstrum and Mahadevan have been omitted for clarity because they lie within a few percent of the solid line.

[17] T. W. Haas and A. G. Jackson, J. Chem. Phys. **44**, 2921 (1966).
[18] R. M. Stern, Appl. Phys. Letters **5**, 218 (1964).
[19] N. J. Taylor, Surface Sci. **2**, 544 (1964).
[20] P. J. Estrup and J. Anderson, J. Chem. Phys. **46**, 567 (1967).
[21] R. E. Schlier, J. Appl. Phys. **29**, 1162 (1958).
[22] J. A. Becker, E. J. Becker, and R. G. Brandes, J. Appl. Phys. **32**, 411 (1961).

with their (100) faces exposed. However, arguing by analogy with tungsten, which is known to have similar surface properties, one would expect adsorbed material to be less strongly bound to the (100) face than to the (110). For example, in the case of O_2 adsorption on tungsten, Germer *et al.*[23] quote 2000°K as the temperature at which O_2 is rapidly desorbed from a (110) face, while Anderson and Danforth[24] note that 1850°K quickly produces a clean (100) LEED pattern from the oxygen covered surface.

Based on the above arguments, we conclude that the surface of a polycrystalline Mo ribbon heated to 2000°K is atomically clean unless carbon impurities are present. The carbon impurity can be removed by heating in O_2, producing an atomically clean surface. This conclusion will be further supported by the γ_i measurements to be reported in the next section.[25]

RESULTS

Initially, the target was cleaned by heating for three days at 1600°K and flashing to 2300°K. Then, γ_i was determined for incident Ar^+ and He^+ ions at ion kinetic energies 50-400 eV. Prior to each measurement, the target was flashed to 2000°K. The results are shown by the solid squares in Figs. 6 and 7. Also shown are the results of Hagstrum[4] and of Mahadevan *et al.*[8] Their experimental points have been omitted from Fig. 7 for clarity since they lie within a few percent of the solid line. The agreement of these results with those of Mahadevan *et al.*, particularly at the higher energies, is striking. For Ar^+, the two sets of data appear to diverge at lower energies; however, the difference is not large and may be regarded as within "experimental error." Equally striking is the large difference for Ar^+ between these results and Hagstrum's.

In order to investigate the possibility of carbon contamination of the target, the target was heated in 1×10^{-6} Torr of oxygen for 30 min at 1700°K. The O_2 atmosphere was pumped out and following several flashes at 2000°K (to remove oxides formed) the values of γ_i shown by the solid circles in Figs. 6 and 7 and in Table I were obtained. Further heating of the target in O_2 did not produce any additional change in the yields. These results are seen to be in excellent agreement with those obtained by Hagstrum.

Over the course of this research we have investigated the electron emission from six different targets all cut from the same piece of Mo foil. In all cases, the values of γ_i obtained lie within 4% of one of the solid lines in Figs. 6 and 7 depending on whether or not the target has been heated in O_2. The 30-min heating time required to clean the target is consistent with the quantitative measurements of carbon depletion rate made by Becker *et al.*[22] for W.

TABLE I. Values of γ_i (electrons/ion) for He^+ and Ar^+ incident on clean polycrystalline Mo.

Ion energy (eV)	He^+		Ar^+	
	This expt.	Hagstrum	This expt.	Hagstrum
50	0.286	0.288	0.127	0.117
100	0.276	0.271	0.125	0.116
150	0.267		0.125	
200	0.263	0.256	0.125	0.116
250	0.261		0.125	
300	0.261	0.252	0.123	0.115
350	0.253		0.123	
400	0.253	0.247	0.123	0.112

Once produced, the higher γ_i values persist under normal target treatment. Allowing the target to stand cold in vacuum or in air does not affect the results, i.e., the yield value after pumping down and flashing to 2000°K is again the high one. However, when the cleaned target was heated for a long period of time (~one day) at 1600°K, the surface carbon was apparently regenerated and γ_i returned to its lower value. This may be due to diffusion of carbon from the normally cool ends of the ribbon to the region of beam-target interaction. In all cases, treatment in O_2 restored the high γ_i value.

DISCUSSION OF RESULTS

The evidence cited in the previous sections leads us to conclude that the differences between the "flashed" and "O_2-heated" results (Figs. 6 and 7) are due to the presence in the former case of carbon impurities on the surface. Mahadevan *et al.* explained the discrepancies between their values and Hagstrum's as due to differences in distributions of crystallite orientations between the targets used. One would expect that differences of this kind would lead to poor reproducibility of data from target to target and even from time to time in the lifetime of a given target. The high degree of reproducibility observed in our experiments tends to discount this explanation. Also in this regard, we have examined the crystallinity of several Mo targets in an x-ray spectrometer. All targets, whether heated in O_2 or not, showed the same general crystal structure. The grain size of heated targets was much larger than the unheated material, the crystallites being visible to the naked eye. In addition, the grains were almost exclusively oriented with the [100] direction within a few degrees of the surface normal. This result is not surprising, since high degrees of orientation have also been reported in the literature for

[23] L. H. Germer, R. M. Stern, and A. U. MacRae, in *Metal Surfaces* (American Society for Metals, Metals Park, Ohio, 1963).

[24] J. Anderson and W. E. Danforth, J. Franklin Inst. **279**, 160 (1965).

[25] The recent work of R. N. Varney, [Phys. Rev. **157**, 116 (1967)] also indicates the presence of carbon on flashed Mo surfaces. In his experiments, Varney observes emission of CN^- ions from a Mo surface bombarded by metastable N_2 molecules. Since no oxygen cleaning was employed, it seems likely that these ions are products of a surface reaction with impurity carbon originating in the bulk of the Mo target. Varney has made a similar observation with a tungsten target (private communication). The author is indebted to Dr. Varney for calling these observations to his attention.

"aged" tungsten ribbons.[26] Note that the occurrence of impurity carbon is not universal, because several LEED experimenters have reported clean-surface patterns without any oxygen treatment.[24] Thus, the apparent absence of any appreciable carbon contamination effects in Hagstrum's work is not anomalous.

Although these experiments are not capable of giving detailed information about surface structure, a few general conclusions can be made regarding the structure of the surface layer and the role of carbon in the Auger emission process. The high degree of reproducibility of the carbon covered results among targets implies that the surface carbon structure is regular rather than "patchy." This is in accordance with the results of Haas and Jackson,[17] who observed well-defined LEED patterns from a carbon contaminated Mo (110) surface.

The magnitude of the effect of the carbon on the Ar^+ yields suggests that the equilibrium density of carbon atoms at the surface must be quite high. In order to examine the manner in which the carbon may affect the Auger emission yields, we tentatively adopt the viewpoint that the carbon may be regarded as a chemisorbed layer on a clean metal surface. An obvious manner in which such a layer would affect the Auger emission yield is through a change in work function ϕ of the surface from the clean-metal value due to the presence of the surface carbon. Hagstrum has considered the effect of such changes in ϕ in the simple form of his theory of Auger emission. He showed that the electron yield is strongly dependent on the quantity $I_p-2\phi$, where I_p is the recombination energy of the ion. Hence the yield for ions of low I_p will be more sensitive to small changes in ϕ. In connection with investigation of the effect of adsorbed layers on Auger emission from tungsten,[6] he has calculated the variation in electron yield to be expected upon changing the work function from 4.5 to 5.0 eV, approximately the variation occuring during adsorption of a monolayer of N_2 on a clean polycrystalline tungsten surface. The results of his calculation are shown in Table II and compared with our experimental results for the clean and carbon-contaminated Mo surface. The calculation neglects the effects of atomic level shifting due to the ion-metal interaction, and thus refers to ion kinetic energies near zero, where this effect is minimized. Hence, comparison is made with our lowest-energy results. The agreement between the calculated differences and our experimental results is good.

We have measured the work function of the contaminated Mo surfaces to substantiate this model. Work functions were determined by a least-squares fit of measurements of thermionic emission current versus target temperature to Richardson's equation. The measurements were made in the following sequence. A new target was installed in the apparatus and was baked and processed as previously described. After this treatment, measurements of γ_i for Ar^+ ions incident produced the lower values (as in Fig. 6), demonstrating that the surface was contaminated. Then thermionic emission data were taken under ultrahigh vacuum conditions, flashing the target frequently to insure that no errors were introduced by adsorption of background gas. The results of these measurements are shown in Fig. 8. The value of ϕ deduced is 4.71 ± 0.18 eV, where the limits stated are the boundaries of the 95% confidence interval. Next, the surface was cleaned by heating in O_2 as previously described. The value of ϕ measured for this surface was 4.28 ± 0.6 eV. The target was then employed in the clean condition in a number of experiments over a period of about two weeks. The apparatus was vented and re-evacuated several times during this period. Following this, the contaminated surface was regenerated as previously described by heating the target at 1600°K for one day. The thermionic emission data taken at this point gave a value of ϕ equal to 4.73 ± 0.20 eV. Finally, the surface was cleaned again by treatment in O_2 and the clean surface work function determined again as 4.33 ± 0.16 eV. The clean-surface data are in excellent agreement with values reported in the literature for polycrystalline Mo and are tabulated in Table III. The measured work-function change of 0.4 eV agrees very well with that expected to produce the observed changes in γ_i on the basis of Hagstrum's calculation.

Considerable additional information concerning the process of Auger ejection can be obtained from measurements of the energy distribution of the ejected electrons. In the present apparatus, such measurements cannot be made with high accuracy since the fringing magnetic field (a few gauss) from the magnetic analyzer is uncompensated in the target region. This results in a distortion of the ejected electron energy distribution, particularly at the lower energies. The energy distributions are most meaningful in the case of He^+, where the analyzing field is the smallest and where the distribution contains a significant number

TABLE II. Effect of work-function change on theoretical and experimental yield values.

	Hagstrum theory (Tungsten)		This experiment W = 50 eV (Molybdenum)	
	$\phi=4.5$ eV	$\phi=5.0$ eV	Clean Mo	Mo+ Carbon
		He^+		
γ_i	0.279	0.250	0.287	0.247
% difference		10.5%		14%
		Ar^+		
γ_i	0.050	0.030	0.126	0.066
% difference		40%		47%

[26] B. J. Hopkins and J. C. Riviere, Proc. Roy. Soc. (London) **81**, 590 (1963).

of high-energy electrons. The electron energy distributions are obtained by differentiating the collector current-voltage characteristic in the region $V_c<0$. Figure 9 shows the results of these measurements. The derivative curves are obtained from the V_c plots by an analog technique. The curves have not been corrected for the effect of work-function difference between target and collector surfaces. This results in an uncertainty of the relative position of the voltage scale for the two curves equal to the work-function change between clean and contaminated surfaces (i.e., about 0.4 eV). The agreement in shape between our clean-surface distribution and that reported by Hagstrum[4] is good, although the broadening effect of the fringe magnetic field is evident. The simple theory of Auger emission predicts that for a change $\Delta\phi$ in work function of the surface (as produced, for example, by an adsorbed layer), the shape of the distribution should be relatively unchanged but the high-energy (leading) edge of the distribution should shift by an amount $2\Delta\phi$. This does not appear to be the case here. Rather, the

TABLE III. Values from literature for work function of clean polycrystalline Mo.

ϕ (eV)	Ref.
4.24	a
4.26	b
4.38	b
4.35	b
4.20	c
4.28	this expt
4.33	this expt

[a] O. K. Husmann, Phys. Rev. **140**, A546 (1965).
[b] Reference 4.
[c] H. B. Michaelson, in *Handbook of Chemistry and Physics* (Chemical Rubber Publishing Co., Cleveland, Ohio, 1964), 45th ed., p. E-43.

shape of the distribution seems to be altered significantly by the presence of the carbon while the base width is unaltered. A detailed analysis of the shape of the energy-distribution curves is outside the intended scope of this paper and is not justified by the accuracy of the data presented here. Analysis of this type is the subject of the recently presented technique of ion neutralization spectroscopy (INS).[7] The methods of INS relate the shapes of the distribution curves to the Auger transition probabilities and ultimately to the density of electronic states in the conduction band of the solid. Suffice it to say that our curves show the same general features as the energy distributions obtained by Hagstrum[6] and by Propst and Luscher[9] for He^+ bombardment of clean and monolayer-covered surfaces of a variety of metals and semiconductors. In particular, surface coverage tends to reduce the number of high-energy electrons while enhancing the low-energy end of the distribution. In the case of monolayer coverage of a clean metal surface by a gas such as N_2 or O_2, it is possible in the analysis of results to argue

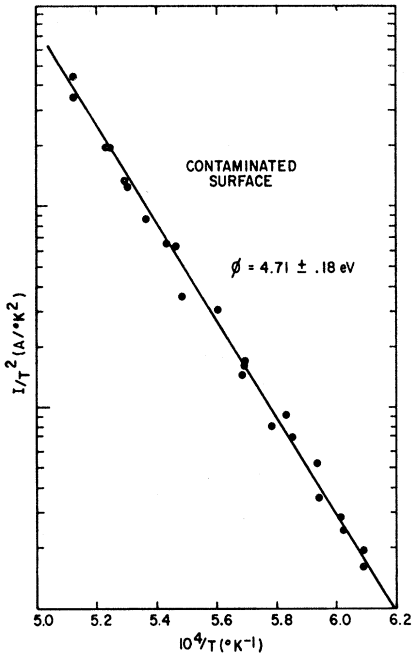

FIG. 8. Richardson plot for carbon-contaminated Mo surface.

that the bulk solid band structure is substantially unaltered by the presence of the adsorbed layer, and hence the changes observed are due to changes in the Auger transition probability. However, in the present case, it must be remembered that the point of view

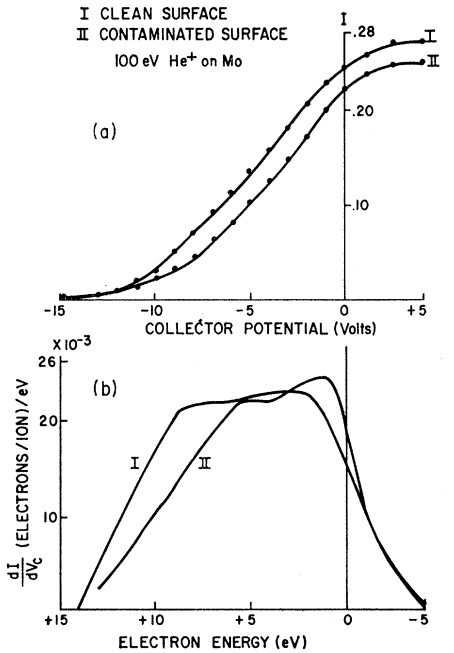

FIG. 9. (a) Detailed plot of retarding portion of collector current voltage characteristic for 100 eV He^+ ions incident on clean (I) and contaminated (II) molybdenum surfaces. (b) Derivatives of curves in (a) giving distribution of energies of ejected electrons for the two surfaces.

that the carbon is a truly surface contaminant is undoubtedly an oversimplification. If, as we have argued, the carbon originates in the bulk of the target ribbon, it is entirely reasonable to suppose that sufficient concentrations of carbon can accumulate in the vicinity of the surface (i.e., the nearest few atomic layers) to cause the density-of-states function there to differ significantly from that for a pure Mo sample. Hence the changes observed in the shapes of the distributions here may reflect changes in bulk band structure as well as Auger transition probability.

SUMMARY

Measurements have been made of the Auger electron emission from polycrystalline molybdenum targets bombarded by He^+ and Ar^+. It has been found that carbon impurities present in the Mo sample reduce the value of the electron yield below that for an atomically clean surface. In accordance with previous work, it was found that the carbon could not be removed from the target by heating in vacuum, but that a short heat treatment in an O_2 atmosphere would remove it, producing an atomically clean surface. This contamination effect is thought to be responsible for some discrepancies in electron yields reported in the literature.

The differences between the Auger electron yields for the clean and carbon-contaminated surfaces can be at least qualitatively explained in terms of an increase of about 0.5 eV in work function of the contaminated surface relative to the clean-surface value. The measured increase of 0.4 eV supports this model. Measurements of the ejected electron-energy distributions for the two surfaces, however, show differences which do not seem interpretable on the basis of this simple model. Rather, it seems that in this case the carbon must be regarded as having a more subtle influence, perhaps involving alterations of the Mo band structure by impurity carbon in the bulk of the sample.

PHYSICAL REVIEW VOLUME 164, NUMBER 2 10 DECEMBER 1967

Landau Damping and Dispersion of Phonon, Plasmon, and Photon Waves in Polar Semiconductors

R. Tsu

IBM Watson Research Center, Yorktown Heights, New York

(Received 19 June 1967)

Landau damping results from the loss of energy of collective motion to the excitation of individual particles. Well known for plasmons, it can also occur for phonons and photons, as is shown herein. For a coupled longitudinal plasmon–optical-phonon wave, it can be significant both near the phonon resonance and near the plasmon resonance. It is generally insignificant for coupled transverse photon–optical-phonon waves. These results are important for infrared spectroscopy and Raman scattering involving plasmons and optical phonons.

I. INTRODUCTION

THE Landau damping of a plasma wave is due to the loss of energy from a collective motion to the individual particles, such as a plasmon decaying by exciting an electron below the Fermi energy. This occurs when the phase velocity of the wave becomes comparable to the thermal speed of the electrons,[1,2] i.e., when the wave number q of the plasmon is comparable to q_{Debye} of the electrons defined by $q_D = (\text{plasma frequency})/v_{\text{thermal}}$. In a coupled system of infrared active longitudinal optical phonons and plasmons, the optical phonons may also decay by exciting electrons. Thus, in addition to the usual optical-phonon loss due to lattice anharmonicity, we have the Landau damping of the optical phonons. The dispersion relations of a coupled system of longitudinal plasma waves and longitudinal optical and acoustic phonons have been examined by Tsu and White.[3] Due to the use of the moment equations of the Boltzmann transport equation, their results do not contain the effects of Landau damping. Varga[4] used the Drude model for the electron gas to derive dispersion relations which include the transverse case, one in which the transverse optical phonons interact with the dressed photons, i.e., photons dressed by electrons. More recently, Singwi and Tosi[5] used the electrostatic interaction Hamiltonian of a longitudinal optical phonon and an electron gas to obtain a dispersion relation similar to Varga's. However, because of the use of a power-series expansion of the dielectric response function in powers of the wave number, their results, like Varga's, also exclude Landau damping. In a coupled system, at frequencies near the optical-phonon resonant frequency, the condition of matching the phase velocity to the thermal speed of the

[1] H. Derfler and T. C. Simonene, Phys. Rev. Letters **17**, 172 (1966).
[2] L. D. Landau, J. Phys. (USSR) **10**, 25 (1946).
[3] R. Tsu and D. L. White, Ann. Phys. (N.Y.) **32**, 1, (1965); **32**, 100 (1965).
[4] B. B. Varga, Phys. Rev. **137**, A1896 (1965).
[5] K. S. Singwi and M. P. Tosi, Phys. Rev. **147**, 658 (1966).